EARLY CHANDRA X-RAY OBSERVATIONS OF ETA CARINAE

F. D. SEWARD, Y. M. BUTT, M. KAROVSKA, A. PRESTWICH. E. M. SCHLEGEL Smithsonian Astrophysical Observatory, 60 Garden St., Cambridge, MA 02138

M. CORCORAN

Laboratory for High Energy Astrophysics, Goddard Space Flight Center, Greenbelt, MD 20771 $Draft\ version\ April\ 26,\ 2024$

ABSTRACT

Sub-arcsecond resolution Chandra observations of η Car reveal a $40'' \times 70''$ ring or partial shell of X-ray emission surrounding an unresolved, bright, central source. The spectrum of the central source is strongly absorbed and can be fit with a high-temperature thermal continuum and emission lines. The surrounding shell is well outside the optical/IR bipolar nebula and is coincident with the Outer Shell of η Car. The X-ray spectrum of the Shell is much softer than that of the central source. The X-ray Shell is irregular and only correlates well with optical features where a bright X-ray knot coincides with a bright feature of the Outer Shell. Implications for the binary model of the central source are discussed.

Subject headings: stars:individual(η Carinae) - stars:early-type - X-rays:stars

1. INTRODUCTION

Eta Carinae has long been an object of mystery, a unique optical variable (see review by Davidson & Humphreys, 1997). Initially of 4th to 2nd magnitude, it brightened to first magnitude in the 1830s and reached a maximum brightness of -1 in 1843. Between 1857 and 1869 it declined steadily from 1st to 7th magnitude. It underwent a second outburst in 1890 (Humphreys, Davidson, & Smith, 1999), declined to and remained at 8th magnitude until about 1940, and has since brightened to almost 5th magnitude (Davidson et al 1999). The central source of Eta Carinae has long been obscured by a small optical nebula, the homunculus, which HST observations have revealed to be a striking bipolar nebula (Hester et al, 1991; Humphreys & Davidson 1994). Measured expansion of the lobes indicate an origin at the time of the "Great Eruption" in 1843 (Walborn et al, 1978). There is also a rapidly expanding disk in the plane between the bipolar lobes which seems to have originated in the later eruption in about 1890 (Smith & Gehrz, 1998). A faint "Outer Shell", with knots of fast-moving material, surrounds the bipolar structure (Walborn 1976).

Eta Carinae is now the brightest extra-solar infrared source at a wavelength of 20 microns. We will use a distance of 2.3 kpc in this paper (Davidson & Humphreys, 1997) but note that most of the previous X-ray work assumed a slightly larger distance of 2.6 kpc. An infrared luminosity of $5\times10^6~\rm L_{\odot}$ was derived by Westphal & Neugebauer (1969) which is only a factor of ≈ 4 less than the optical luminosity during the Great Eruption (Davidson & Humphreys, 1997). It is now believed that the source of energy is a massive object, or objects, at the center and that surrounding dust then re-radiates the energy in the infrared. Indeed, infrared emission is observed to come from the bipolar nebula and the equatorial disk (Smith et al, 1998). The central source, however, remains obscure at optical and infrared wavelengths.

Since X-rays can penetrate dust, the X-ray band holds the promise of revealing more of the central object. The first convincing observation was with Einstein (Chlebowski et al 1984). This showed emission from an unresolved source in the vicinity of the central object and from an irregular outer region. This structure was confirmed with ROSAT observations by Corcoran et al (1995) who discovered that the central source was variable. The Einstein spectrum was interpreted as the sum of a hard, stronglyabsorbed component and a soft component. A later observation with ASCA (Corcoran et al, 1998) showed the same dual nature and, with the better ASCA energy resolution, emission lines from Mg, Si, S and Fe were detected in the spectrum. Neither the Einstein IPC nor the ASCA SIS instruments could spatially resolve the central source from the surrounding shell. A campaign to monitor high energy X-rays with XTE has been in progress since April 1996. The variability observed is remarkable, showing a possible 85 day periodicity and a 3-month X-ray minimum (Ishibashi et al, 1999). These results have been interpreted with a model invoking colliding stellar winds and a massive binary system (Corcoran et al, 2000b).

2. CHANDRA OBSERVATIONS

 η Car was one of the first science observations done with Chandra (Weisskopf, O'Dell, & VanSpeybroeck 1996). To demonstrate the capability of the observatory, Eta Carinae was observed on 7 September 1999 with the Chandra ACIS-I detector, first in TE (timed exposure) mode for 10,800 s, then in CC (continuous clocking) mode for 12,200 s. During this period (and unbeknownst at the time) the energy resolution of the detector was degrading significantly as a result of radiation damage. Although the energy resolution of these spectra is considerably better than the present capability of the instrument, the calibration for this period of rapidly-changing characteristics is poor.

ring or shell of soft emission with dimension $\sim 40'' \times 70''$ surrounds a bright central source. It is open in the south and lies closer to the central source in the west than in the east. There are two bright knots. Emission from the ring is soft whereas the spectrum of the central source is hard and strongly absorbed. At energies below 1.0 keV, only the ring is seen.

The geometry and weakness of interior diffuse emission indicate a geometry more ring-like than shell-like. The orientation of this material, however, does not have a sensible relationship to the geometry of the bipolar nebula. The ring, e.g., is not in the equatorial plane where it might first be expected. The most likely possibility is that we are seeing clumps of material in an irregular shell so we will refer to this material as the (Outer) Shell, but will use a partial torus to calculate the density.

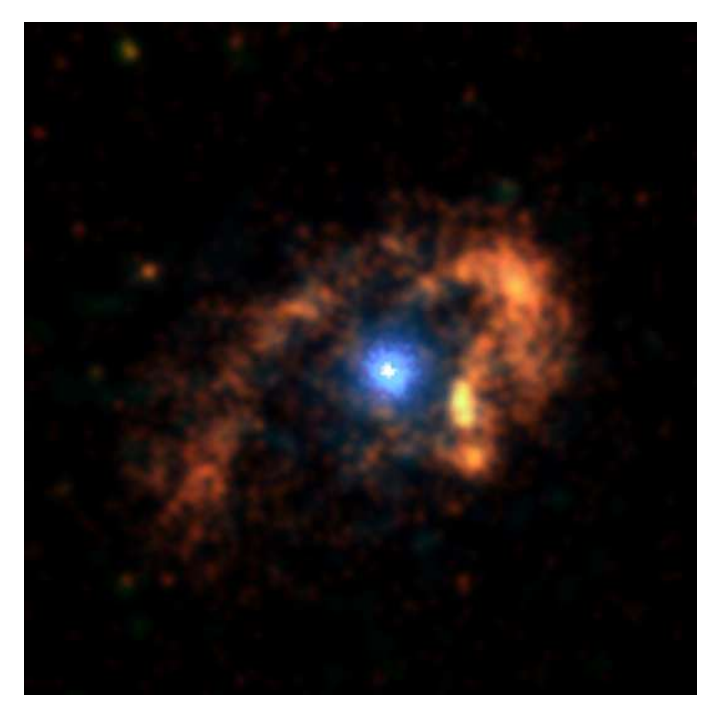


Figure 1:Contours of 2.1-8.0 keV surface brightness overlaid on a 6590Å HST image of η Car printed to show the Outer Shell. Contour spacing is proportional to the square root of the surface brightness. The bright X-ray source is coincident with the central source of the bipolar nebula. Closely-spaced contours around this source indicate scattering from the telescope mirror but the faintest contour partially follows the the Outer Shell.

Figure 1 was made using an adaptive smoothing algorithm (CSMOOTH) to post-process the η Car images. This smooths a two-dimensional image in such a way that the smoothing scale is increased until the total number of counts under the kernel exceeds a value that is determined from a preset significance and the expected number of background counts in the kernel area. The scale is determined by convolving the raw image with a Gaussian kernel whose size grows from a small initial value to the maximal allowable value corresponding to the size of the raw image itself.

Data were analyzed using the Chandra CIAO software

and the FTOOLS XSPEC. Both TE and CC mode data were first cleaned by rejecting ACIS event-grades 1,5, and 7 ('Chandra Proposers' Observatory Guide, 2000). Since η Car is a bright source we did not do any background filtering. The ACIS focal-plane temperature at the time of the observation was -100° C. Since no calibration has vet been done for this temperature, we used spectral response matrices for -90° and shifted the gain so the model spectrum reproduced the observed Ir (the mirror coating) absorption edge at 2.1 keV. The observed spectral structure indicates that the resolution is close to that observed in the -90° calibrations. the gain shift was also checked against a better-known Cas A spectrum taken a few days earlier. The lack of calibrated response matrices, however, prevents an accurate spectral analysis, particularly at low energies.

3. COMPARISON WITH BIPOLAR NEBULA AND OUTER SHELL

Figure 2 shows 0.1-0.8 keV X-ray emission superimposed on the HST WFPC image (courtesy Jon Morse) with the F658N filter. This filter is centered at 6590 Å, and passes [NII] lambda 6583 and scattered H-alpha (Morse et al., 1998). X-ray emission from the central source is strongly absorbed, so only the extended soft emission from the Shell is visible. Note that there are no X-ray features corresponding with the bright optical bipolar nebula. The extended X-ray Shell is, instead, clearly associated with compact knots of line emission described by Morse et al (1998) as being in the "Outer Debris Field", which is the same region as Walborn's "Outer Shell". The brightest X-ray knot coincides exactly with a bright optical patch in the SW Outer Shell (Walborn's "S condensation"). The X-ray maximum which forms the NW part of the Shell is at the outer boundary of the Debris Field (the "W arc") and the maximum at the SE extreme of the X-ray Shell coincides with the SE extension of the Debris Field (the "E condensations").

Figure 3 shows a higher energy band; here 2.1-8.0 keV X-ray brightness contours are superimposed on the same F658N image. The central source now dominates the X-ray image but there is also a hint of emission from the Outer Shell. This will be discussed in Section 6.

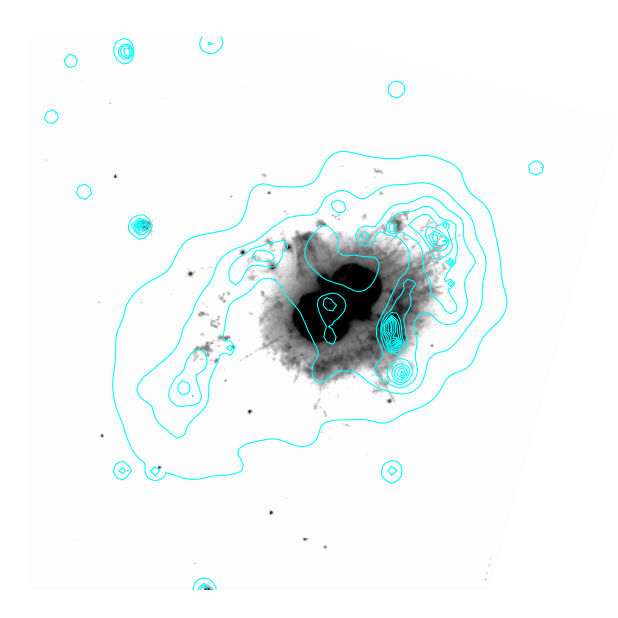


Figure 2: The soft X-ray ring overlaid on a 6590 Å HST image of η Car printed to show the Outer Shell. The X-ray ring is clearly associated with the ragged optical knots which form the Outer Shell. The brightest X-ray knot coincides with the brightest optical knot southwest of the central source. Contour spacing is proportional to the square root of the surface brightness.

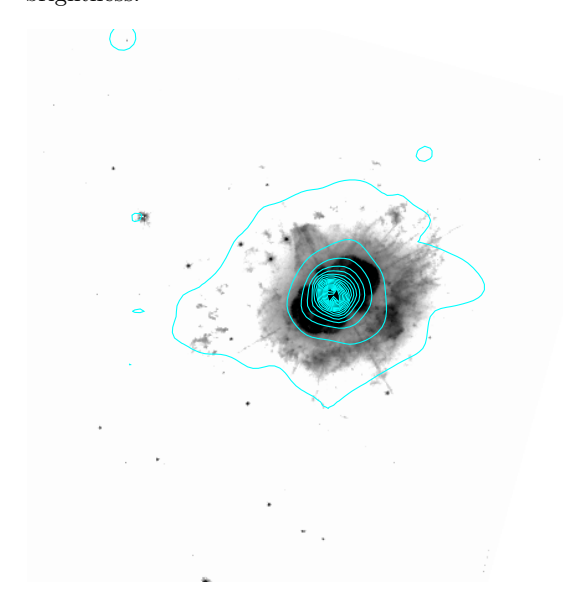


Figure 3: Contours of 2.1-8.0 keV surface brightness overlaid on a 6590Å HST image of η Car printed to show the Outer Shell. Contour spacing is proportional to the square root of the surface brightness. The bright X-ray source is coincident with the central source of the bipolar nebula. Closely-spaced contours around this source indicate scattering from the telescope mirror but the faintest contour partially follows the the Outer Shell.

4. THE CENTRAL SOURCE

The central source has a strength of 1.6 counts s⁻¹ in the CC mode observation. The TE-mode data, with apparent rate 0.17 s^{-1} , is severely distorted by "pileup", a phenomenon where 2 or more photons register in a single ACIS pixel during its recording interval and are counted as one event having the summed energy of all interacting

photons in that pixel. The flux measured at the detector is 4.4×10^{-11} erg cm⁻² s⁻¹ and, at 2.3 kpc distance, the source luminosity (before absorption in surrounding material and ISM) is $L_X = 6 \times 10^{34}$ erg s⁻¹ in the range 0.2-10 keV. Flux calculations using the PIMMS program (CXC et al,2000) are given in Table 1.

Figure 4 shows the pulse-height spectrum of the central source. Since there is no exact calibration, the energy scale is still uncertain. If the Ir edge at 2.1 keV is used to determine the energy, the energy of the prominent Feline emission is in the range 6.5 to 6.8 keV. With this normalization, the general shape of the spectrum is well reproduced using either a power law or a thermal continuum. There are emission lines at energies 2.4 (S), 3.7-4.0 (Ca), and 6.5-6.8 (Fe) keV. If the calibration assumed reproduces the detector response reasonably, there may also be lines at 1.3 (Mg), 1.9 (Si), and 3.2 (A) keV. An absorption of 4×10^{22} atoms cm⁻² of cold material is required. The continuum fit is not sensitive to temperature in the range kT = 6-20 keV. If a Raymond model is used, the Fe emission line shape seems to require a strong contribution from Fe XXV and/or Fe XXVI at ≈ 6.8 keV and kT of ~ 15 keV, although both XTE and ASCA spectra indicate a temperature of $\sim 5 \text{ keV}$ (Corcoran et al., 2000a).

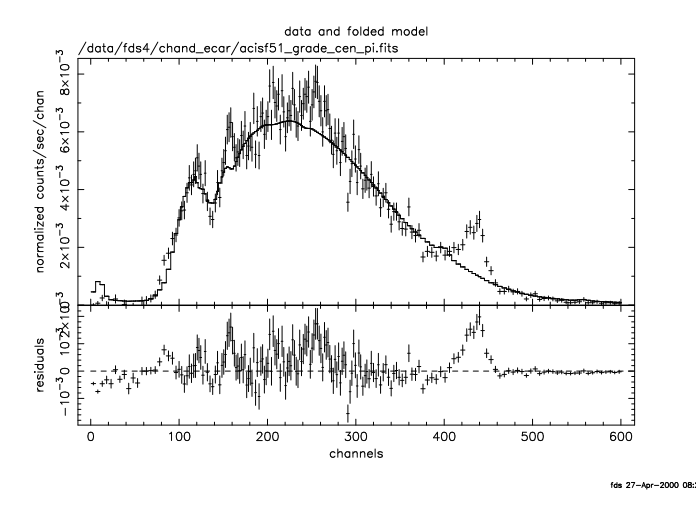


Figure 4: X-ray spectrum of the central source taken from the CC-mode data. Spectrum is fit with a Bremsstrahlung continuum with kT=15 keV. The notch at channel 140 (2.1 keV) is an absorption edge in the Ir mirror coating. There is a broad Fe emission line at channel 440 (≈ 6.7 keV) and evidence for emission lines at lower energies. There is no emission below 1.0 keV.

The broad Fe line emission requires at least two components at ~ 6.8 and ~ 6.5 keV. This is consistent with the report of Corcoran et al (1998) of an Fe fluorescence line at ~ 6.4 keV in the ASCA data. A deeper Chandra observation is planned with the grating and a well-calibrated ACIS configuration so we will not elaborate here on the detail of these line emissions.

The appearance of the central source in the TE data (Figure 1) suggests a surrounding halo of scattered X-rays. Figure 5 shows the Chandra point-response function

(prf) compared to the radial surface brightness of the central source. The prf has been weighted according to the measured spectrum and normalized to the counting rate measured in the CC observation. Since pileup is most severe in pixels with highest counting rate, the central surface brightness is greatly diminished, but there is no distortion apparent at radial distances > 2.5''. The surface brightness follows the prf closely from 2.5 to 5'' radius, so we conclude that there is no observable scattering halo at these radial distances. Even excluding energies below $1.0~{\rm keV}$, some emission remains at larger radial distances. The faintest contour in Figure 3 follows the morphology of the Outer Shell indicating some emission from material in this area.

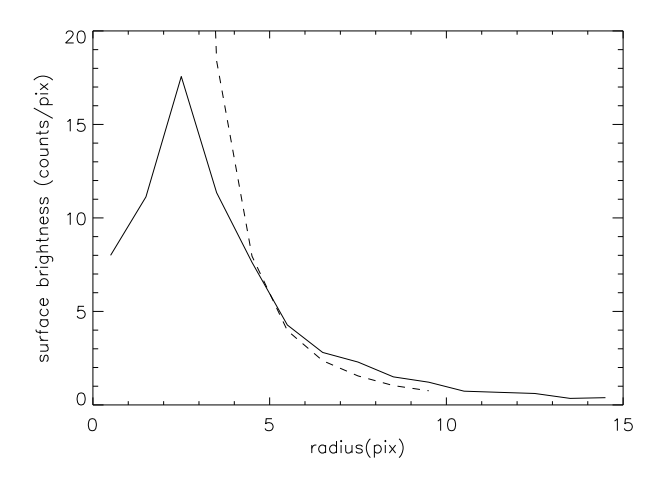


Figure 5: The radial surface brightness of the central source compared to a weighted Chandra point-source response function. The solid line is the data, greatly depressed at the center because of pileup. Dashed curve is the prf which has intensity of 10,000 at the source position. One ACIS pixel = 0.5".

The line of sight to the central source passes through the SE (nearer) lobe of the bipolar nebula (Morse et al., 1998). The path length inside this lobe is $\approx 10^{17}$ cm so the observed X-ray-absorbing column of 4×10^{22} atoms cm⁻² implies a density of $\approx 4\times 10^5$ atoms cm⁻³ inside the lobe. This is in good agreement with other estimates (Davidson and Humphreys, 1997). As the lobe expands, and if no more material is injected, the X-ray absorbing column should decrease with time.

5. THE OUTER SHELL

The emission is soft. At energies above 2 keV the Shell almost disappears (note the faint residual seen in Figure 3). The central source obscures any high-energy diffuse emission which might come from the central region.

The geometry is more ring-like than shell-like. The projection of a limb-brightened shell would have more central emission. A shell with thickness 1/5 the radius would have central brightness $\approx 40\%$ of the brightest part of the limb. We observe only $\approx 15\%$. For the analysis, we assume a ring (torus) with diameter 45'' = 0.50 pc and thickness (diameter of circular cross-section) 7'' = 0.08 pc. The ring is inclined 45° - 50° from the plane of the sky and 1/4 of

the ring is missing. Volume of this partial ring is 1.7×10^{53} cm³. The brightest knot of emission has projected dimension $4'' \times 6''$ and, assuming an intermediate thickness, the volume is 2.6×10^{51} cm³.

The spectrum of the Shell was obtained by extracting events from an elliptical region including the Shell and excluding events from the central source. This spectrum shown in Figure 6 is a rather smooth continuum with some structure from 0.6 to 0.9 keV. This can be fit with a bremsstrahlung continuum with kT ranging from 0.2 to 0.4 keV and with lines at ~ 0.4 and ~ 0.7 keV, perhaps from N and Fe L. A Raymond model with cosmic abundances predicts line emission from Ne at ~ 0.9 and from Mg at ~ 1.3 which are not evident in the spectrum. We are not being precise here because the calibration uncertainty increases at low energies. Both effective area and energy scale are not well-calibrated so the existence and identification of spectral features is highly uncertain. Nevertheless, a low energy feature in ASCA spectra was also found by Tsuboi et al (1997) and by Corcoran et al (1998) which they identified as due to N. If this is really a N emission line, the low transmission of the ISM at ~ 0.4 keV implies that the Shell is remarkably bright in N emission, an appealing thought since some of the optical knots shine brightly with N line emission (Davidson et al, 1982; Davidson et al., 1986). The X-ray spectrum of the bright knot is, within the statistics of the ≈ 400 counts collected, the same as that of the whole Shell.

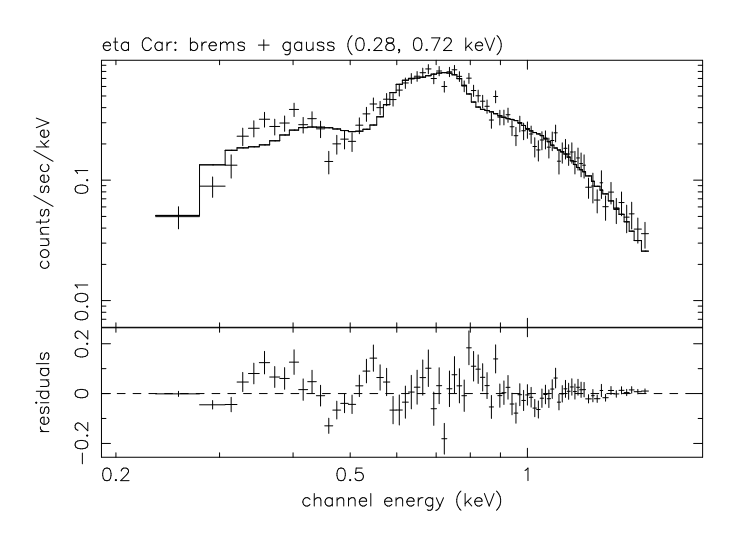


Figure 6: X-ray spectrum of the ring. Spectrum is fit with a Bremsstrahlung continuum with kT=0.21~keV and with 2 emission lines with energies ≈ 0.3 and 0.7 keV.

The X-ray flux from the Shell is 2.2×10^{-12} erg cm⁻² s⁻¹, measured at the detector and which, using kT = 0.3 and N_H = 2×10^{21} atoms cm⁻², implies an X-ray luminosity, $L_X = 1.0 \times 10^{34}$ erg s⁻¹. Assuming a uniform density throughout the torus, we calculate a density of 50 atoms cm⁻³. Total thermal energy is 2×10^{46} ergs. Total mass is 1.0×10^{-2} M_{\odot}. The bright knot contains 4×10^{-4} M_{\odot} at a density of 130 atoms cm⁻³.

Davidson et al (1986) estimated the amount of UVemitting material in the S condensation as $\sim .02 M_{\odot}$ with electron density of $\sim 10^4$. The X-ray emitting gas in the bright knot thus represents only 1% of the material in this region.

Even though the morphology is not convincingly shell-like, could this material be a limb-brightened shell of hot gas behind a blast wave originating in the Great Eruption 160 years ago? The answer is yes. The age of a blast wave can be calculated from the radius and temperature (e.g. Seward & Velusamy, 1995) and the result is 185^{+105}_{-70} years which is consistant with the time since the Great Eruption.

An alternate way of heating the X-ray emitting gas is via the optical knots in the Debris Field. These have velocities of 300-1300 km s⁻¹ (Walborn, Blanco, and Thackeray 1978) implying ejection (with no deceleration) 130-900 years ago. The hot gas in the Shell could be pre-existing material heated by energy deposited by these fast-moving knots, some of which may have originated in the Great Eruption. Gas temperature and knot velocity are consistant with this process. Indeed, all the knots may have been ejected in 1843 (or even later) with high velocities but have since been decelerated in the Outer Shell, some more than others.

The optical knots show strong line emission which is thought to be due to shocks – either from high velocity knots colliding with interstellar clouds or a fast wind impacting on cometary knots of material. The X-ray emitting gas is compatable with either process.

6. APPLICATION TO MODEL OF THE CENTRAL SOURCE

This Chandra observation has confirmed, in a satisfactory way, the two-component model used to explain all observations since that of Einstein; two components, soft and hard, with only the harder radiation coming from the near vicinity of the central object. We now compare the 2-10 keV Chandra data with that of XTE which has been used to define a promising model of the central source.

A square degree of sky containing η Car has been monitored since May 1997 with XTE (Corcoran, et al, 2000b). The 2-10 keV flux observed varies, usually smoothly, from 5 to 16×10^{-11} erg/cm⁻² s⁻¹ with some fluctuations at high intensity. There is also a 3-month minimum, interpreted as an eclipse, during which the flux drops, not to zero, but to a minimum of 0.5×10^{-11} erg/cm⁻² s⁻¹. ASCA spectra obtained from a 3' diameter region during this time yield a flux of 5.7×10^{-11} erg/cm⁻² s⁻¹ (2-10 keV) in the "high" state and 0.43×10^{-11} erg/cm² in the low, eclipsed state (Corcoran, et al., 2000a). If this 2-10 keV emission observed during the eclipse is from η Car itself, it has a significant impact on the model.

The currently-proposed model ascribes the 2-10 keV X-ray flux to shocked emission from a wind-wind collision in a massive binary system. In this binary model (Corcoran et al. 2000b), at the time of the Chandra observation, the wind-wind collision shock is about 15 AU $\approx 7 \times 10^{-3}$ arcsec from the more massive star, and so would be unresolved to Chandra. As noted by Corcoran et al. (2000a) the ASCA X-ray spectrum of η Car during the X-ray

low state in 1997.9 is inconsistent with the colliding wind binary model since the colliding wind source should be completely hidden during the eclipse (which is caused by absorption in the wind from the primary star). Perhaps, the 2-10 keV emission seen by ASCA at that time is produced by another source of hard emission in the ASCA extraction region (a circle of 3' radius around η Car). We can search for this in the Chandra data.

The 2-10 keV flux measured by Chandra in CC mode (Fig. 4) is $4.4\times10^{-11}\,\mathrm{erg/cm^{-2}\,s^{-1}}$ and is almost all from the vicinity of the central source. A near-simultaneous observation with XTE (Corcoran, et al 2000) measures $6\times10^{-11}\,\mathrm{erg/cm^{-2}\,s^{-1}}$. This discrepancy probably illustrates the uncertainty in absolute flux measured by different instruments. No other significant sources of 2-10 keV emission are seen in the field. There are, however, at least 50 weak serendipitous sources (almost all are stars in the cluster Tr16) within 5' of η Car. There is also weak diffuse emission above 2 keV observed from the Outer Shell which is well within the region covered by ASCA.

In the range 2-10 keV, we observe a small bright halo around the central source which is due to the telescope point response function. Assuming that the flux from η Car does not vary between the CC and TE mode observations, the 2-10 keV diffuse flux at radial distances greater than 10" is in excess of that expected in the "wing" of the telescope point response function.

In an annulus defined by radii 10'' and 90'', in the 2-10 keV band, the observed count rate is 5.5% that of the central source. The Chandra mirror PRF indicates that mirror scattering should be $\approx 3.5\%$. The 9 brightest serendipitous sources account for 0.2% so there is a residual diffuse emission intrinsic to the region with strength $\approx 2\%$ that of the central source or about 8×10^{-13} erg cm⁻² s⁻¹. The ASCA-measured residual during eclipse minimum was \approx 5% of the maximum source strength. We conclude that, although half of the ASCA-measured eclipse residual might be diffuse, the other half must come from a region very close to η Car, within a Chandra resolution element of $\sim 0.5''$ or within ~ 1000 AU of the central star. Speckle interferometry from the ground (Weigelt and Ebersberger 1986) and direct imaging from space (Morse et al. 1998) have revealed the presence of starlike knots, the Weigelt Blobs, within 0.4'' from η Carinae; it is possible that scattering of the colliding wind emission by one or more of these knots produces the 2-10 keV emission seen in the ASCA low state spectrum, and may be also responsible for the Fe fluorescent line detected in the ASCA spectra. It is also possible that the X-ray emitting region is not completely eclipsed and the model needs to account for this.

Acknowledgments: We thank Roberta Humphreys for helpful suggestions and for pointing out several vital references, thus saving us the embarassment of seeming to ignore work which defines the nature of this peculiar object. Financial support was provided by the Chandra X-ray Center NASA Contract NASS-39073.

Table 1 COUNT RATE, FLUX, AND LUMINOSITY

		Energy Range	Central Source	Ring
ACIS Rate	counts s^{-1}	0.2-10 keV	1.6 ± 0.1	$0.40 \pm .01$
kT	keV	_	15^{+5}_{-10}	0.3 ± 0.1
N_H	${\rm atoms~cm^{-2}}$	-	4×10^{22}	2×10^{21}
Flux (absorbed)	${\rm erg~cm^{-2}~s^{-1}}$	0.2-10	$4.4^{+0.0}_{-0.7} \times 10^{-11}$	$2.2 \pm 0.3 \times 10^{-12}$
Flux (unabsorbed)	${\rm erg~cm^{-2}~s^{-1}}$	0.2-10	$8.8 \pm 0.3 \times 10^{-11}$	$1.5^{+1.7}_{-0.5} \times 10^{-11}$
Flux (absorbed)	${\rm erg~cm^{-2}~s^{-1}}$	2-10	$4.3^{+0.0}_{-0.7} \times 10^{-11}$	-
L_X (No ISM absorption)	${ m erg~s^{-1}}$	0.2-10	$2.8^{+0.0}_{-0.5} \times 10^{34}$	$1.0^{+1.1}_{-0.6} \times 10^{34}$
L_X (No η Car absorption)	${\rm erg~s^{-1}}$	0.2-10	$5.6 \pm 0.2 \times 10^{34}$	-

REFERENCES

Chandra X-ray Center, Chandra Project Science, IPI Teams, 2000, "Chandra Proposers' Observatory Guide", TD 403.00.02,

Chandra X-ray Center, Cambridge, MA Chlebowski, T., Seward, F.D., Swank, J., Szymkowiak, A., 1984, ApJ 281, 665

Corcoran, M.F., Rawley, G.L., Swank, J.H., Petre, R., 1995, ApJ 445, L121.

Corcoran, M.F., Petre, R., Swank, J.H. Drake, S.A., Koyama, K., Tsuboi, Y., Viotti, R., Damineli, A., Davidson, K., Ishibashi, K., White, S., Currie, D., 1998, ApJ 494, 381.

Corcoran, M.F., Fredericks, A.C., Petre, R., Swank, J.H., Drake,

S.A., 2000a, ApJ, in press. Corcoran, M.F., Ishibashi, K., Swank, J.H., Petre, R., 2000b, ApJ, submitted.

Davidson, K., Walborn, N.R., Gull, T.R., 1982, ApJ 254, L47 Davidson, K., Dufour, R.J., Walborn, N.R., Gull, T.R., 1986, ApJ

Davidson, K., Humphreys, R.M., 1997, ARA&A 35, 1.

Davidson, K., et al, 1999, AJ 118, 1777. Hester et al, 1991, AJ 102, 654.

Humphreys & Davidson, 1994, PASP 106, 1025 Humphreys, R.M., Davidson, K., Smith, N., 1999, PASP 111, 1124. Ishibashi, K., Corcoran, M.F. Davidson, K., Swank, J.H., Petre, R., Drake, S.A. Damineli, A., White, W., 1999, ApJ 524, 983. Morse, J., Davidson, K., Bally, J., Ebbets, D., Balick, B., Frank, A.,

1998, AJ, 116, 2443 Seward, F. D. & Velusamy, T., 1995, ApJ 439, 715

Smith, N., Gehrz, R.D., Krautter, J., 1998, ApJ 116, 1332.
Smith, N., Gehrz, R.D., 1998, ApJ 116, 823.
Tsuboi, Y., Koyama, K., Sakano, M. & Petre, R., 1997, PASJ, 49,

Walborn, N.M 1976, ApJ 204, L17.
Walborn, N.M., Blanco, B.M., Thackeray, A.D. 1978, ApJ 219, 498.
Weigelt, G., & Ebersberger, J, 1986, AA 163, L5.
Weisskopf, M.C., O'Dell, S.L., Van Speybroeck, L.P. 1996, Proc. SPIE, 2805, 2.